VOL. 15, NO. 11, JUNE 2020 ISSN 1819-6608
ARPN Journal of Engineering and Applied Sciences

www.arpnjournals.com

CHARACTERIZATION OF TRILINEAR FLOW REGIME IN FRACTAL SHALE RESERVOIRS

Freddy H. Escobar[1], Ruthsandy Barón-Morela[1] and Daniel Suescún-Díaz[2]
[1]Petroleum Engineering Department, Universidad Surcolombiana, Avenida Pastrana - Cra 1, Neiva, Huila, Colombia
[2]Departamento de Ciencias Naturales, Avenida Pastrana, Universidad Surcolombiana, Neiva, Huila, Colombia
E-Mail: fescobar@usco.edu.co

ABSTRACT

This paper presents the analysis of pressure tests in unconventional reservoirs from the trilinear model of anomalous diffusion based on fractal geometry and anomalous diffusion in order to simulate the heterogeneity of flow in the reservoir in order to be able to obtain a flow prediction approximate to the real. Based on this model, we generate curves in which by applying the *TDS* methodology, new equations to determine reservoir parameters such as internal reservoir permeability, hydraulic fracture permeability, fracture conductivity, and reservoir dimensions are created. Likewise, through the input of the parameter alpha (α) four cases are defined, which show the variation of the flow depending on the connection between its elements. Finally based on data obtained from the literature, pressure tests were simulated in order to verify the right operation of the equations and that are within the error tolerance range.

Keywords: multilinear flow, fractal theory, trilinear model, anomalous diffusion, *TDS* technique.

1. INTRODUCTION

The trilinear flow was developed by Brown et al. (2009) as an analytical model that describes the behavior of a complex system formed by a hydraulically fractured horizontal well connected to an internal reservoir with natural fractures and an external reservoir in a non-conventional shale reservoir. This model takes as reference point works previously developed by other researchers whose base was the introduction of the Laplace transform by Van Everdigen and Hurst (1949) for the solution of models that are based on the Diffusivity Equation in porous media. Brown *et al.* (2009) uses the dual porosity transient (Kazemi, *et al.*, 1969) and pseudo steady-state dual porosity (Warren and Root, 1963) models to provide a solution to the Laplace transform in naturally fractured deposits which allows the modeling of the internal reservoir, in the same way, based on the model developed by Raghavan *et al*. (1997), the solution is given for a pressure transient for multiple fractured horizontal wells, managing to model the behavior of hydraulic fractures.

Recently, Raghavan and Chen (2016) provided an anomalous diffusion model which is related to the fractal nature of the fracture network where certain coefficients for the heterogeneous porous medium are presented. Two common approaches to modeling naturally fractured reservroirs are used, that of discrete fracture connection (DFN) (Araujo et al. 2004) and dual porosity. In the DFN it is possible to consider the details of each fracture, the distribution and the connectivity of the network, the model requires extensive characterization studies and because of the roughness of calculations they lead to computational models being inefficient, therefore, the details that can be used by these models are limited by the capabilities of the flow models, which leads to these methods being eligible for routine engineering applications.

Dual porosity models are based upon continuous and average assumptions of fracture properties, where the material contained in the primary porosity is homogeneous and isotropic and is contained in an identical arrangement of rectangular parallelepipeds, and the flow can occur between the elements of primary and secondary porosity, but not among the elements of primary porosity (Warren & Root, 1963). The model is appropriate for homogeneous systems where there are repeated patterns of continuous fractures that allow determining a predominant flow, however, if the variations in fractures, connectivity and conductivity of fractures are considered, it is only a first degree approximation, to the behavior of the networks in the horizontal wells.

TDS has shown to be of powerful application on fractal reservoirs. Escobar, Lopez-Morales and Gomez (2015) presented the first *TDS* formulation for naturally-fractured fractal reservoirs. The formulation offered by the *TDS* Technique cannot be performed with the straight-line conventional analysis. Escobar, Salcedo and Pinzon (2015) extended *TDS* methodology for power-law fluids in homogeneous fractal reservoirs.

This investigation, uses the *TDS* technique in order to generate characteristic "finger prints" that allow us to obtain equations to characterize the different flow regimes, the concepts of anomalous diffusion and fractal geometry are introduced, to make the calculations less extensive and to simulate the heterogeneity of flow velocity in the system and in this way to obtain a behavior closer to the real one.

2. MATHEMATICAL BACKGROUND

The anomalous diffusion model (T_{DA}) developed by Ozcan *et al.* (2014) replaces the double porosity model (T_{DP}) with a model in which a porous medium with fractal geometry and anomalous diffusion is considered, this in order to obtain a behavior that has a greater adjustment to the real behavior of the deposits.

2.1 Trilinear Flow Model

The basis of the trilinear flow model is the premise that the productive life of a horizontal well with

multiple fractures is dominated by linear flow regimes. The trilinear flow model groups linear flows into three continuous regions of flow: the outer reservoir (denoted with the subscript O), the inner reservoir located between artificial fractures (denoted with subscript I), and the hydraulic fracture (denoted with the subscript F). In this model it is assumed that the internal reservoir is naturally fractured and that the hydraulic fractures are of finite conductivity with a uniform distribution throughout the horizontal well, Brown *et al.* (2009).

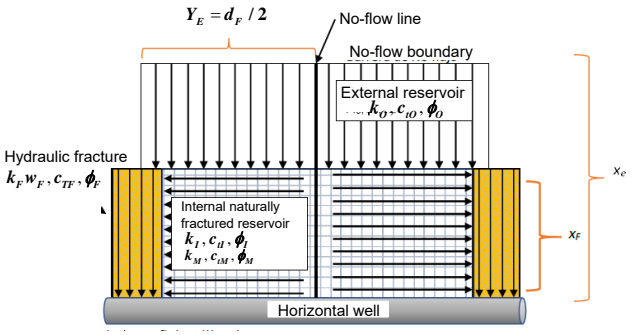

Figure-1. Trilinear Flow system schematic, after Ozkan *et al.* 2009).

2.2. Fractal Geometry

Fractal geometry developed by the mathematician Mandelbrot (1982), is based on the hypothesis that an irregular object is formed of small fragments that resemble the whole and have similar characteristics, many petrophysical properties that affect the flow in the porous medium, show fractal characteristics. Naturally fractured deposits were generally simulated by the Warren and Root (1963) two-scale model, in which, the fracture network is represented by Euclidean geometry, therefore, to represent these networks of different scales and with non-behavioral behavior. Euclidean fractal geometry was proposed as a solution. Chang and Yortsos (1990), propose a fractal system in a naturally fractured porous medium where fractals (Fractures) are located within a Euclidean geometry (Matrix), in which it is assumed that flow storage occurs in a local volume, which each fracture has the same density and the number of fractures to be simulated is taken into account.

2.3 Abnormal Diffusion in Porous Media

Unlike conventional reservoirs in which the Darcy flow dominates, in unconventional shale formations, where there are low permeabilities and are heterogeneous reservoirs, it has been shown that a diffusive flow is more accurate when representing the flow behavior in place, Kuchuk and Biryukov (2015), Poon 1998). Diffusion is the result of the Brownian movement, which is the random movement resulting from the collision between molecules in a liquid, solid or gaseous medium. The relationship between the squared displacement of the particle and time is represented by the diffusivity coefficient (α), where a normal diffusion occurs when α = 1 and at values less than one there is a sub-diffusion. Normal diffusion is usually associated with homogeneous deposits with a constant flow, where the squared displacement of the particle is a linear function with time. In unconventional reservoirs there is a sub-diffusion, where the coefficient (α) is directly related to the heterogeneity of the deposit. The smaller α becomes, the velocity of the reservoir becomes more heterogeneous and the movement of the fluid is constantly interrupted.

2.4 Mathematical Model

For simplicity of calculations in the trilinear model, the terms are presented in a dimensionless manner. The definition of the pressure drop is given by the following formulae:

$$P_D = \frac{\lambda_I h_I}{141.2qB}\Delta P \tag{1}$$

For gas reservoirs:

$$m(P_D) = \frac{\lambda_I h_I}{1422.54\, q_{Fsc} T}\Delta m(P) \tag{2.a}$$

$$\left(t_D * m(P_D')\right) = \frac{kh}{141.2q\mu B}\left(t * \Delta m(P')\right) \tag{2.b}$$

Where q_{Fsc} is the flow rate of each individual fracture that is equal to the total horizontal well flow divided by the number of hydraulic fractures:

$$q_{Fsc} = \frac{q_{sc}}{n_f} \tag{3}$$

The dimensionless pressure derivative is given by:

$$\left(t_D * P_D'\right) = \frac{kh}{141.2q\mu B}\left(t * \Delta P'\right) \tag{4}$$

The dimensionless time is given by:

$$t_D = 2.637\times10^{-4}\frac{\eta_I}{x_F^2}t \tag{5}$$

Where t is the time in hr, x_F is the average length of hydraulic fracture in ft and η_I is the diffusivity of the internal reservoir defined by:

$$\eta_I = \frac{\lambda_I}{(\phi C_t)_I} \tag{6}$$

$$\lambda_I = \frac{k_I}{\mu} \tag{7}$$

Equations (1) and (5) correspond to the dimensionless pressure and dimensionless time of the trilinear dual-porosity model. For the trilinear diffusion-anomalous model, η_I and λ_I refers to η_α and λ_α, where k_I =

k_α, and k_α is different from the conventional Darcy permeability. The distance (ξ_D) and the dimensionless thickness of the Hydraulic fracture (w_{FD}) are also defined, respectively:

$$\xi_D = \frac{\xi}{x_F} \tag{8}$$

Where ξ is the distance in X or Y. The dimensionless thickness is defined by:

$$w_{FD} = \frac{w_F}{x_F} \tag{9}$$

w_F is the width of the hydraulic fracture. The dimensionless conductivities of the reservoir and the fracture are defined by:

$$C_{FD} = \frac{k_F w_F}{k_I x_F} \tag{10}$$

$$C_{RD} = \frac{k_I x_F}{k_O Y_E} \tag{11}$$

Being k is the permeability in md, $k_F w_F$ is the hydraulic fracture conductivity in md-ft and Y_E is the reservoir size in the y-direction y given in ft.

The diffusivity radii of the hydraulic fracture and the external reservoir are given by:

$$\eta_{FD} = \frac{\eta_F}{\eta_I} \tag{12}$$

$$\eta_{OD} = \frac{\eta_O}{\eta_I} \tag{13}$$

Where η refers to the diffusivity in part of the reservoir, Equation (6). The term of density of natural fractures is introduced:

$$\rho_f = \frac{n_f}{h} \tag{14}$$

3. *TDS* TECHNIQUE FORMULATION

Different pressure and pressure derivative behaviors where generated with the T_{DA} model proposed by Ozcan *et al.* (2014. Once the input data was entered, variables were modified in order to identify those that would change the behavior of the pressure derivative. With this exercise it was concluded that the most influential variable in the behavior of the reservoir is α, followed by the average length of the fracture (x_F), reservoir size in the y-direction (Y_E), permeability of the internal reservoir (k_I) and fracture permeability (k_F). In the analysis of the behavior of the pressure derivative and identification of sensitivities, it was observed that the dominant variable in the flow variation in the reservoir was α, which causes a reaction of the pressure derivative modifying its behavior, and showing four cases.

3.1 Case 1 (α = 0.1 - 0.2)

A linear flow of slope 0.5 is observed, which represents the flow in the fracture, followed by a pseudo steady-state flow that identifies the time in which the matrix no longer provides flow to the natural fractures, refer to Figure-2.

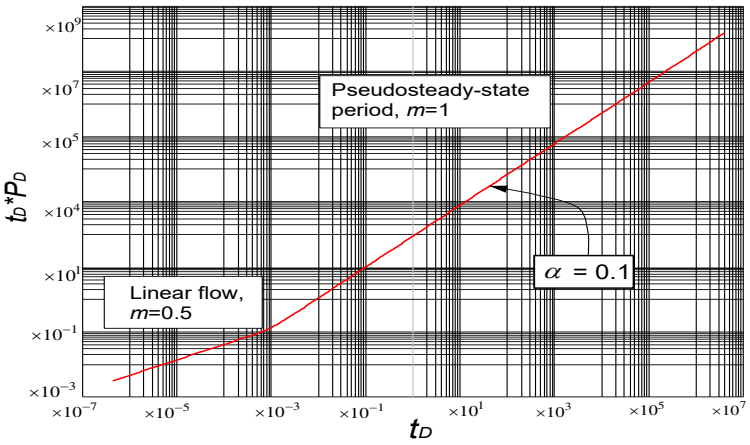

Figure-2. Pressure derivative behavior for case 1.

3.2 Case 2 (α= 0.3-0.4) and Case 3 (α= 0.5-0.9)

In the second case case a multilinear flow of slope 0.3 is observed, followed by a second multilinear flow of slope 0.8 and finally a pseudo steady-state period of unit slope. (α = 0.3-0.4) as depicted in Figure-3. In the third case, a multilinear flow of slope 0.3 is presented at early times, followed by a second multilinear flow of slope 0.6 and later a pseudo steady-state period of unit slope. (α = 0.5 - 0.9) (Figure-4).

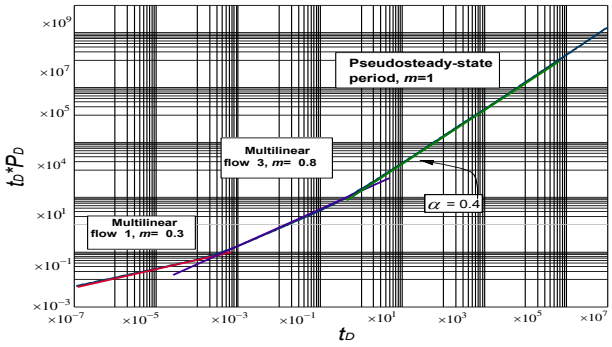

Figure-3. Pressure derivative behavior for case 2.

3.3. Case 4 ($\alpha = 1$)

The fourth case is presented at values of $\alpha = 1$, at early times a bilinear flow is identified ($m = 0.25$), followed by a linear flow ($m = 0.5$) and ends with a pseudo steady-state period of unit slope. In this case the flow in the fracture networks is not hindered by the matrix, since the system is densely fractured and efficiently connected, therefore, the system will be depleted more quickly with better efficiently, which causes the fractures natural dominate the flow in the reservoir and that the flow between the reservoir and the fracture of finite hydraulic conductivity begins at early times forming a bilinear flow. (Figure-5).

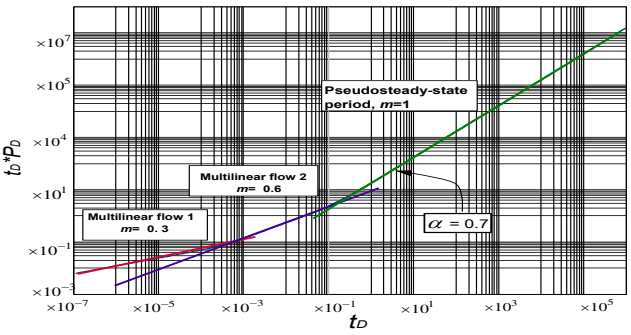

Figure-4. Pressure derivative behavior for case 3.

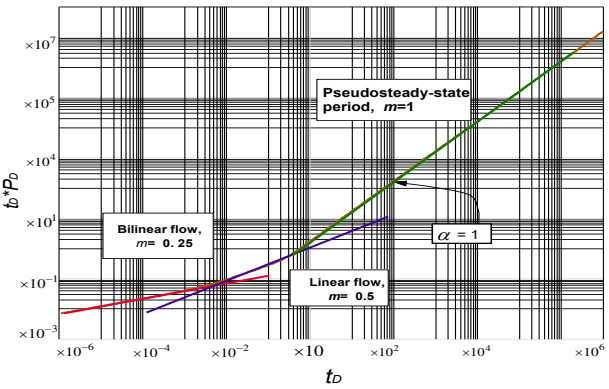

Figure-5. Pressure derivative behavior for case 4.

Once the cases and sensitive variables were identified, the curves were adjusted and the governing equation of each of the flows was developed, after which the desired variable was solved in each of the equations taking into account the equations raised in the mathematical model of Ozkan *et al*. (2014). The resulting equations are given in Table-1.

Additionally, the intersection between the different flow regimes were used to solve for some reservoir parameters as pointed out by Tiab (1995). These equations are provided in Table-2.

Table-1. *TDS* Equations for gas and oil cases.

Flow Regime & Equation numbers	Governing Equation	Oil case	Gas case
Linear (15-19)	$\left(t_D * P_D{}'\right)_L = 1.08\left(\frac{t_{D_L}}{\alpha^2}\right)^{0.5}$	$k_I = 2\pi \frac{t_L \mu}{\phi ct}\left(\frac{qB}{h\left(t^*\Delta P'\right)_L x_F \alpha}\right)^2$ $S_L = \frac{\pi}{179\alpha}\left(\frac{\Delta P_L}{\left(t^*\Delta P'\right)_L} - 2\right)\sqrt{\frac{k_I t_L}{\phi\mu c_t x_F^2}}$	$k_I = 622.4\left(\frac{q_{F,sc}T}{h\left(t^*\Delta \mathrm{m}(P)'\right)_L}\right)^2\left(\frac{t_L}{\phi c_t \mu x_F^2 \alpha^2}\right)$ $S_L = \frac{\pi}{179\alpha}\left(\frac{\Delta m(P)_L}{\left(t^* m(\Delta P)'\right)_L} - 2\right)\sqrt{\frac{k_I t_L}{\phi\mu c_t x_F^2}}$
Bilinear (20-24)	$\left(t_D * P_D{}'\right)_{BL} = 0.16\left(\frac{t_{D_{BL}} k_F w_F}{k_I y_E}\right)^{0.25}$	$k_F w_F = \frac{\phi ct x_F^2 y_E}{69\mu^3 t_{BL}}\left(\frac{k_I h\left(t^*\Delta P'\right)_{BL}}{qB}\right)^4$ $S_{BL} = \frac{\pi}{154}\left(\frac{\Delta P_{BL}}{\left(t^*\Delta P'\right)_{BL}} - 4\right)\left(\frac{t_{BL}}{\phi\mu c_t {x_F}^2}\frac{k_F w_F}{y_E}\right)^{0.25}$	$k_F w_F = \frac{2.41\times10^{-6}}{\mu^3}\left(\frac{k_I h\left(t^*\Delta m(P)'\right)_{BL}}{qT}\right)^4\left(\frac{\phi c_t x_F^2 Y_E}{t_{BL}}\right)$ $S_{BL} = \frac{\pi}{154}\left(\frac{\Delta m(P)}{\left(t^*\Delta m(P)'\right)_{BL}} - 4\right)\left(\frac{t_{BL}}{\phi\mu c t {x_F}^2}\frac{k_F w_F \alpha}{Y_E}\right)^{0.25}$
Multilinear 1 (25-29)	$\left(t_D * P_D{}'\right)_{m1} = 0.3\left(\frac{t_{D_{m1}} k_F w_F}{k_I h\alpha}\right)^{0.3}\left(t^*\Delta P'\right)_{m1}$	$k_F w_F = \frac{\pi}{214}\left(\frac{k_I\left(t^*\Delta P'\right)_{m1}}{qB}\right)^3\left(\frac{\phi c_t x_F^2 \alpha}{t_{m1}}\right)\left(\frac{h^2}{\mu}\right)^2$ $S_{m1} = \frac{\pi}{124}\left(\frac{\Delta P_{m1}}{\left(t^*\Delta P'\right)_{m1}} - 3.33\right)\left(\frac{t_{m1}}{\phi\mu c t {x_F}^2}\frac{k_F w_F}{h\alpha}\right)^{0.3}$	$k_F w_F = \frac{\pi}{214}\frac{\phi ct\mu {x_F}^2 \alpha}{t_{m1}}\left(\frac{k_I\left(t^*\Delta m(P)'\right)_{m1}}{qT}\right)^3 h^4$ $S_{m1} = \frac{\pi}{124}\left(\frac{\Delta m(P)_{m1}}{\left(t^*\Delta m(P)'\right)_{m1}} - 3.33\right)\left(\frac{t_{m1}}{\phi\mu c t {x_F}^2}\frac{k_F w_F}{h\alpha}\right)^{0.3}$
Multilinear 2 (30-34)	$\left(t_D * P_D{}'\right)_{m2} = 2.7\left(\frac{t_{D_{m2}} x_F^{0.7}}{Y_E^{0.7}\alpha^{0.7}}\right)^{0.6}$	$k_I = 12.2\left(\frac{q\mu B}{h\left(t^*\Delta P'\right)_{m2}}\right)^{2.5}\left(\frac{t_{m2}}{\phi\mu c_t x_F^{1.3} Y_E^{0.7}\alpha^{0.7}}\right)^{1.5}$ $S_{m2} = \frac{1}{51.9}\left(\frac{\Delta P_{m2}}{\left(t^*\Delta P'\right)_{m2}} - 1.7\right)\left(\frac{t_{m2}}{\phi\mu c_t x_F^{1.3}}\frac{k_I}{\alpha^{0.7}Y_E^{0.7}}\right)^{0.6}$	$k_I = 3911.9\left(\frac{qT}{h\left(t^*\Delta m(P)'\right)_{m2}}\right)^{2.5}\left(\frac{t_{m2}}{\phi\mu c_t x_F^{1.3} Y_E^{0.7}\alpha^{0.7}}\right)^{1.5}$ $S_{m2} = \frac{1}{51.9}\left(\frac{\Delta m(P)_{m2}}{\left(t^*\Delta m(P)'\right)_{m2}} - 1.7\right)\left(\frac{t_{m2}}{\phi\mu c_t x_F^{1.3}}\frac{k_I}{\alpha^{0.7}Y_E^{0.7}}\right)^{0.6}$
Multilinear 3 (35-39)	$\left(t_D * P_D{}'\right)_{m3} = 31\left(\frac{t_{D_{m3}} x_F \alpha}{Y_E}\right)^{0.8}$	$k_I = 7770.02\left(\frac{q\mu B}{\left(t^*\Delta P'\right)_{m3} h}\right)^5\left(\frac{t_{m3}\alpha}{\phi\mu c t x_F Y_E}\right)^4$ $S_{m3} = \frac{\pi}{74}\left(\frac{\Delta P_{m3}}{\left(t^*\Delta P'\right)_{m3}} - 1.25\right)\left(\frac{t_{m3}}{\phi\mu c t x_F}\frac{\alpha}{Y_E}\right)^{0.8}$	$k_I = 1.24\times10^{-7}\left(\frac{qT}{\left(t^*\Delta m(P)'\right)_{m3} h}\right)^5\left(\frac{t_{m3}\alpha}{\phi\mu c t x_F Y_E}\right)^4$ $S_{m3} = \frac{\pi}{74}\left(\frac{\Delta m(P)_{m3}}{\left(t^*\Delta m(P)'\right)_{m3}} - 1.25\right)\left(\frac{t_{m3}}{\phi\mu c_t x_F}\frac{\alpha}{Y_E}\right)^{0.8}$
Pseudo steady (40-42)	$\left(t_D * P_D{}'\right)_{pss} = 1.21\frac{t_{D_{pss}} x_F}{Y_E \alpha}$	$x_F = 0.045\frac{qB}{h}\frac{t_{pss}}{\phi c_t Y_E \alpha\left(t^*\Delta P'\right)_{pss}}$	$x_F = 0.45\frac{qT}{h}\frac{t_{pss}}{\phi\mu c_t Y_E \alpha\left(t^*\Delta m(P)\right)_{pss}}$

Table-2. Intersection time equations.

Intercept between	Equation	Equation Number
Linear-bilinear	$k_F = 0.91\frac{k_I{}^2 Y_E t_{BLLi}}{\alpha^4\phi c_t \mu w_F x_F^2}$	(43)
Multilinear 2-pseudosteady	$Y_E = \frac{8.52\times10^{-4}\alpha^{0.72}}{x_F^{0.34}}\left(\frac{k t_{m2pssi}}{\phi c_t \mu}\right)^{0.68}$	(44)
Multilinear 1-Multilinear 3	$k_F = 1.57\times10^{-4}\left(\frac{w_F}{h}\right)^{0.3}\left(\frac{Ye}{\alpha^{1.37}}\right)^{0.8}\frac{\phi c_t \mu x_F^{1.2}}{k_I^{1.3} t_{m1m3i}}$	(45)
Multilinear 3-pseudosteady	$Y_E = \frac{2.07\times10^{-6}}{x_F{}^{0.2}\alpha^9}\left(\frac{k_I t_{m3pssi}}{\phi ct\mu}\right)$	(46)
Linear-pseudo steady	$Y_E = 1.9\times10^{-2}\left(\frac{k_I t_{Lpssi}}{\phi ct\mu}\right)^{0.5}$	(47)
Multilinear 1-Multilinear 2	$k_F = \frac{0.047 h t_{m1m2i}}{\mu c_t \phi w_F}\left(\frac{k_I}{x_F^{0.3}}\right)^2\left(\frac{Y_E^{-0.7}}{\alpha^{0.2}}\right)^2$	(48)

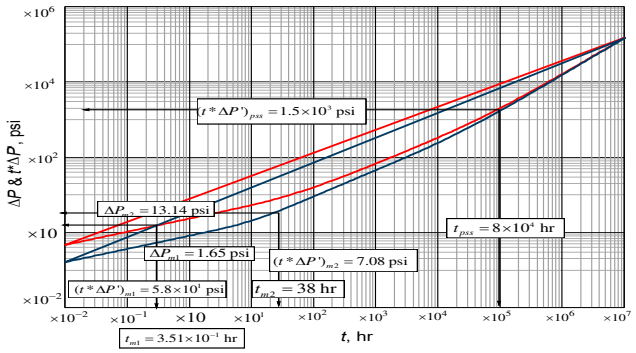

Figure-6. Pressure and pressure derivative versus time for worked example.

4. EXAMPLE

To verify and apply the equations presented in Tables-1 and -2, the Barnett field data presented by Brown *et al*. (2009), Table-3, were used to generate synthetic pressure and pressure derivative behavior and then apply the developed equations once the characteristic points are read. The generated data are plotted in Figure-6.

Table-3. Input data for worked example.

Parameter	Value	Parameter	Value
α	0.6	$k_{\alpha, md}$	0.13
x_e	275	$k_{O,\ md}$	1x10^{-6}
$Y_{E,\ ft}$	90.3	$(\phi c_t)_{\alpha,\ psi}{}^{-1}$	2 x10^{-4}
$x_{F,\ ft}$	150	ϕ_F	0.38
$w_{F,\ ft}$	0.01	$c_{tF,\ psi}{}^{-1}$	1 x10^{-4}
$h,\ _{ft}$	300	ϕ_O	0.04
$r_{w,\ ft}$	0.25	$\mu,\ _{CP}$	0.3
$k_{F,\ md}$	10000	$q_{F,stb/d}$	150

Solution. The current flow regimes are identified in Figure-6 and it is evidenced that the case presented is 3, where at an early time there is a multilinear flow m = 0.3, followed by a second multilinear flow of m = 0.6 and finally a pseudo steady-state period. The following characteristic points were read from this plot:

Multili-near (m=0.3)	t_{m1}	**0.351**	ΔP_{m1}	**1.65**	$(t^*\Delta P')_{m1}$	**0.58**
Multili-near 2 (m=0.6)	t_{m2}	0.68	ΔP_{m2}	13.14	$(t^*\Delta P')_{m2}$	7.08
Pseudo-steady	t_{pss}	8000	ΔP_{pss}		$(t^*\Delta P')_{pss}$	1500

Intersection points:

t_{m1m2i}	**15**
t_{m2pssi}	16000

The fracture conductivity is determined with Equation (26) for the multilinear flow, m = 0.3 is:

$$k_F w_F = \frac{\pi}{214}\left(\frac{0.13\times 0.58}{150\times 1.43}\right)^3 \times \left(\frac{2\times 10^{-4}\times 150^2\times 0.6}{0.351}\right)\times\left(\frac{300^2}{0.02}\right)^2$$

$k_F w_F$ = 99.32 md-ft

The skin factor of this flow regime is obtained with Equation (27):

$$S_{m1} = \frac{\pi}{124}\left(\frac{1.65}{5.8\times 10^{-1}} - 3.33\right)\left(\frac{0.351\times 100}{2\times 10^{-4}\times 0.02\times 300\times 0.6\times 150^2}\right)^{0.3}$$

S_{m1} = 0.043

The remaining calculation results are given in Table-4.

Table-4. Comparative results for the worked example.

Parameter/ Eq. number	Actual value	This study	Error(%)
$k_F w_F$, md-ft (26)	100	99.32	0.68
k_I, md (32)	0.13	0.139	6.9
x_F, ft (41)	150	158	5.3
k_F, md (48)	10000	9914.2	0.9
Y_E, ft (44)	90.3	90.7	0.44

5. CONCLUSIONS

a) Through the anomalous diffusion trilinear flow model and the application of the *TDS* technique, it was possible to develop expressions to characterize a trilinear configuration reservoir considering the flow heterogeneity and interconnection between its elements. The expressions were successfully tested with several examples, although only one is presented.

b) With the implementation of α, a heterogeneous flow was simulated, and it was identified as the most influential variable in the behavior of the pressure derivative and in order of the flows.

c) Four cases originated by the configuration of the system were identified, the contribution of each of its elements and the diffusivity of these in the porous medium, the presence of these cases with the variation of the flows demonstrates the versatility presented by the model to simulate different scenarios with complex reservoir forms and heterogeneous velocity flows, making a more realistic prediction possible, without the need for extensive studies of characterization and roughness of calculations.

d) In cases 1, 2 and 4 an α value located between the ranges specified for each case can be applied. The variation of the results will be minimal and will comply with the permissible error range. For case 3 - being the widest range of values- it is suggested that for a more precise calculation α is solved for some of the equations based on values obtained by petrophysical interpretations and data obtained from the reservoir.

Nomenclature

A	Reservoir area, ft^2
B_o	Oil volume factor, rb/STB
B_g	Gas volumen factor, ft^3 /SCF
C_{RD}	Dimensioneless hydraulic fracture conductivity
C_t	Total compressibility, 1/psi
d_F	Distance between two adjacent hydraulic fractures, ft
h	Reservoir thickness, ft
h_f	Natural fractures thickness, ft
h_{ft}	Total natural fractures thickness, ft
h_m	Matrix thickness, ft
k	Permeability, md
k_I	Internal reservoir permeability, md
k_f	Permeability of natural fractures, md
k_F	Permeability of hydraulic fracture
k_o	External reservoir permeability, md
k_α	Phenomenological coefficient of anomalous diffusion, md
k_m	Matrix permeability, md
$m(P)$	Pseudopressure, psi^2/cp
m	Slope
n_F	Number of hydraulic fractures
n_f	Number of natural fractures
P	Pressure, psi
P_D	Dimensionless pressure
q	Flow rate, STB/D
$q_{F,sc}$	Flow rate per hydraulic fracture, oil STB/d, gas Mscf/d
r_w	Wellbore radius, ft
S	Skin factor
t	Time, hr
t_D	Dimensionless time
$t_D{*}P'_D$	Dimensionless pressure derivative
$t_D{*}\ m(P)'_D$	Dimensionless pseudopressure derivative
$t{*}\Delta m(P)$	pseudopressure derivative, psi^2/cp
w_F	Hydraulic fracture width, ft
x_e	Reservoir lenght, in x-direction, ft
x_F	Hydraulic fracture half length, ft
Y_E	Reservoir lenght, in y-direction, ft
Griego	
α	Difussivity coefficient
$\alpha_{O,F}$	Parameter defined in the trilinear flow model
$\beta_{O,F}$	Parameter defined in the trilinear flow model
Δ	Drop, change
ϕ	Porosity, fraction
η	Difusivity, ft^2 /hr
λ	Mobolity, md/cp
μ	Viscosity, cp
ρ	Density, lb/ft^3
ξ	Mdium type: I, F, O
ω	Storativity coefficient
Sufijos	
D	Dimensionless
e	External boundary
f	Natural fracture
F	Hydraulic fracture
i	Intercept
I	Internal
m	Matrix
O	External reservoir
R	Reservoir
sc	Standard conditions
BL	Bilinear
L	Linear
pss	Pseudosteay-state
$m1$	Multilinear 1
$m2$	Multilinear 2
$m3$	Multilinear 3

REFERENCES

Araujo H., Lacentre P., Zapata T., Del Monte A., Dzelalija F., Gilman J. and Ozkan E. 2004, January 1. Dynamic Behavior of Discrete Fracture Network (DFN) Models. Society of Petroleum Engineers. doi:10.2118/91940-MS.

Bourdarot G. and Balvet B. B. 1998. Well testing: Interpretation methods. Paris, France: Editions Technip.

Brown M. L., Ozkan E., Raghavan R. S. and Kazemi H. 2009, January 1. Practical Solutions for Pressure Transient Responses of Fractured Horizontal Wells in Unconventional Reservoirs. Society of Petroleum Engineers. doi: 10.2118/125043-MS

Chang J. and Yortsos Y. C. 1990, March 1. Pressure Transient Analysis of Fractal Reservoirs. Society of Petroleum Engineers. doi:10.2118/18170-PA.

Escobar F. H., Lopez-Morales L. and Gomez K. T. 2015. Pressure and Pressure Derivative Analysis for Naturally-Fractured Fractal Reservoirs. Journal of Engineering and Applied Sciences. 10(2): 915-923.

Escobar F. H., Salcedo L. N. and Pinzon C. 2015. Pressure and pressure derivative analysis for fractal homogeneous reservoirs with power-law fluids. Journal of Engineering and Applied Sciences. 10(11): 4763-4772.

Kazemi H. 1969. Pressure transient analysis of naturally fractured reservoirs with uniform fracture distribution. Society of petroleum engineers Journal. 9(04): 451-462.

Kuchuk F. and Biryukov D. 2015. Pressure-transient tests and flow regimes in fractured reservoirs. SPE Reservoir Evaluation & Engineering. 18(02): 187-204.

Mandelbrot B. B. 1982. The fractal Geometry of. Nature. 394-397.

Ozkan E., Brown M. L., Raghavan R. S. and Kazemi H. 2009, January 1. Comparison of Fractured Horizontal-Well Performance in Conventional and Unconventional Reservoirs. Society of Petroleum Engineers.

Ozcan O., Sarak H., Ozkan E. and Raghavan R. S. 2014, October 27. A Trilinear Flow Model for a Fractured Horizontal Well in a Fractal Unconventional Reservoir. Society of Petroleum Engineers. doi: 10.2118/170971-MS.

Poon D. 1995, January 1. Transient Pressure Analysis of Fractal Reservoirs. Petroleum Society of Canada. doi: 10.2118/95-34.

Raghavan R. S., Chen C.-C. and Agarwal B. 1997, September 1. An Analysis of Horizontal Wells Intercepted by Multiple Fractures. Society of Petroleum Engineers. doi: 10.2118/27652-PA.

Raghavan R., Chen, C.-C. and Agarwal B. 2019, April 22. Evaluation of fractured rocks through anomalous diffusion. Society of Petroleum Engineers. doi: 10.2118/195305-PA.

Van Everdingen A. F. and Hurst W. 1949. The application of the Laplace transformation to flow problems in reservoirs. Journal of Petroleum Technology. 1(12): 305-324.

Warren J. E. and Root P. J. 1963, September 1. The Behavior of Naturally Fractured Reservoirs. Society of Petroleum Engineers. doi: 10.2118/426-PA.